# Core-valence interactions in Cr and Fe 2p photoemission

C. Bethke* and E. Kisker

*Institut für Angewandte Physik, Universität Düsseldorf, D-40225 Düsseldorf, Germany*

N. B. Weber

*Focus GmbH, Am Birkhecker Berg 20, D-65510 Hünstetten, Germany*

F. U. Hillebrecht

*Institut für Festkörperforschung, Forschungszentrum Jülich, D-52425 Jülich, Germany*

The magnetic linear dichroism (MLDAD) in Fe 2p photoemission spectra of an epitaxial ultrathin iron film has been determined. The experiment reveals multiplet related spectra, which allow a detailed characterization of the photoemission process in a simple final state model, that emphasizes the core-valence interaction in Fe 2p photoemission. The same model was used to describe the Cr 2p photoemission spectrum of Cr adsorbates on a Fe surface. The importance of the investigations for the discussion of the 2p photoelectron spectra of 3d metals is pointed out.

## I. INTRODUCTION

Core level photoemission spectra of magnetic materials may carry information on the magnetic ground state in two ways: first, in the spin polarization of the photoelectrons,[1] caused by exchange interaction between the core hole spin and the magnetically ordered valence electrons, and second, by the occurrence of magnetic dichroism in the spectra.[2] Magnetic dichroism is a spin-averaged dependence of the photoemission line shape on the relative orientation of sample magnetization, light polarization, and electron emission direction. One of the key problems for an adequate description of these effects is the treatment of the interaction between the core hole and the magnetically ordered valence electrons.

Two different approaches may be envisaged for the description of 2p photoelectron spectra of 3d metals, either a single particle picture or an atomic-like model, where the valence electrons are localized. In both models the spin-orbit splitting $\zeta(2p)$ is dominant and so the 2p core level can be described in $jj$ coupling. In the single particle approach,[3–7] the effect of the magnetic valence electrons is described as an effective magnetic field, leading to a Zeeman-like splitting of the main lines according to the magnetic quantum number $m_j$. For emission out of a $p$-level, this leads to four sublevels for the $j=3/2$ final state and for two sublevels for the $j=1/2$ final state. The splitting depends on the ground state magnetic moment, represented by the so called "spin field"[3] obtained by solving the spin-polarized Dirac equation. The coupling between the total angular momentum $j$ of the core hole and $J$ of the "open" valence shells is not taken into account.

The alternative atomic approach describes the ground state by a distinct configuration, e.g. Fe atoms as $3d^6 4s^2 (^5D_4)$ in its Hund's rule ground state,[8] or fcc Ni as a linear combination of a few different configurations $3d^n$ with $n=8\dots10$, and considers all dipole allowed transitions to final states of the type $(2p^5 3d^n)^+ + \epsilon s, \epsilon d$. In contrast to the photoionization of atoms, the core hole $2p^{-1}$ in the 2p shell of metals is screened by an additional valence charge attracted to the ionized site. For example the 2p photoemission spectra of thin fcc Ni films were discussed in various final-state models, e. g. the ligand-field multiplet model,[8] cluster-model,[9,10] and final-state impurity model.[11,12] Notably the single particle model based on fully relativistic polarized Korringa-Kohn-Rostoker (SPR-KKR) Green's function method fails completely to describe the Ni 2p photoemission.[13] In previous papers Dürr *et al.*[14] studied the 2p photoemission spectra of Mn and Fe systems to demonstrate the different effects of electron correlation on photoemission from itinerant or localized magnets. In this context, the limited suitability of the ground state one electron model has been pointed out.

The question arises if a modified atomic approach can explain the spin polarization and the dichroism in 2p photoemission of localized and itinerant magnets. In order to address this question we have studied the MLDAD of the 2p photoelectron spectra from Cr and Fe and we will show that both spectra can be described by a simple final state model.

## II. EXPERIMENTAL

The measurements of the 2p photoemission spectra were performed at the undulator beamline BW3 at HASYLAB. The direction of easy magnetization for Fe on W(110) is along the in-plane $\langle \bar{1}10 \rangle$ direction for thicknesses up to 70 Å, and changes to the $\langle 001 \rangle$ direction above this thickness. To ensure that the easy axis is in the $\langle 001 \rangle$ direction already for a 12 to 15 monolayer (ML) Fe film, samples were grown epitaxially on 3 ML Cr on W(110) by electron beam evaporation, following the procedures described by Gradmann *et al.*[15] The base pressure was $1 \times 10^{-8}$ Pa, the pressure remained in the range of $3 \times 10^{-8}$ Pa during deposition from high purity Fe and Cr rods, with a typical deposition rate of 1.5 and 0.5 Å/min, respectively. The thickness of the deposit

was monitored by a quartz crystal oscillator. Valence band spectra were measured to control the surface cleanliness during the experiment. An analysis of low-energy electron diffraction (LEED) patterns ensured epitaxial growth of the thin films. The thickness of the Fe film is large enough to eliminate any Cr $2p$ photoelectron signal of the 3 ML intermediate Cr layer. The easy axis for magnetization is along the in-plane $\langle 001 \rangle$ direction of the Fe(110). The thin film samples were magnetized by current pulses through coils close to the sample. The magnetic state of the thin Fe film sample can be assumed to be single domain after applying field pulses of about 80 Oe. All data were taken in remanence of the Fe film. Studies of the magnetic moments of Cr adsorbates in the thickness range up to 1 monolayer on Fe(110) and Fe(100) by photoemission studies[16] showed an antiferromagnetic coupling of the Cr adsorbate with the remanent magnetized Fe film.

The linearly $p$-polarized radiation was incident under 45° measured to the surface $\langle \bar{1}10 \rangle$ direction. Photoelectrons were recorded in normal emission with geometrical acceptance of the spectrometer entrance lens of about 8° full cone with relatively large kinetic energy ($>100$ eV), to ensure that possible photoelectron diffraction features (see Henk *et al.*[6]) were averaged out. The experimental geometry is sketched in the inset of Fig. 1(a). All experiments were performed at room temperature.

The total energy resolution, including the finite energy spread of the photons, was about 0.5 eV measuring the Fe $2p$ photoelectron spectra and about 0.6 eV measuring the Cr $2p$ spectra.

### III. RESULTS AND DISCUSSION

In general a direct comparison between the core-level photoemission spectra of free $3d$ metal atoms and thin $3d$ metal films is misleading, because in most cases the ground state differs and the valence electrons in $3d$ metals are itinerant. However, for the special case of Cr and Mn an approach based on the analogy of atomic spectra and spectra from ultrathin films appears to be a reasonable starting point.[17] This is caused by the fact that the valence electrons of Cr and Mn atoms in Hund's rule ground state have no angular momentum ($L_0 = 0$) and Cr or Mn surface compounds are very localized.[14,16]

In order to compare the magnetic dichroism, the thin film must be magnetized and the free atoms must be oriented (the magnetic sublevels $m_J$ of the Hund's rule ground state must be populated asymmetrically).[17–20]

#### A. Cr $2p$ photoemission

So far only the $2p$ photoemission spectra of a magnetized Cr surface layer on 12 ML Fe/Cr/W(110) have been compared to the spectra of free laser-oriented Cr atoms.[17] The spectra and the magnetic dichroism based on a single configuration approximation (Cr$^+2p^53d^44s$) is well reproduced by Hartree-Fock calculations in intermediate coupling. The resulting coefficients $B_{k_0 k k_\gamma}$ contain the many-electron dipole matrix elements $\langle \gamma_f J_f, \epsilon l j : J \| D \| \gamma_0, J_0 \rangle$ and describe the dy-
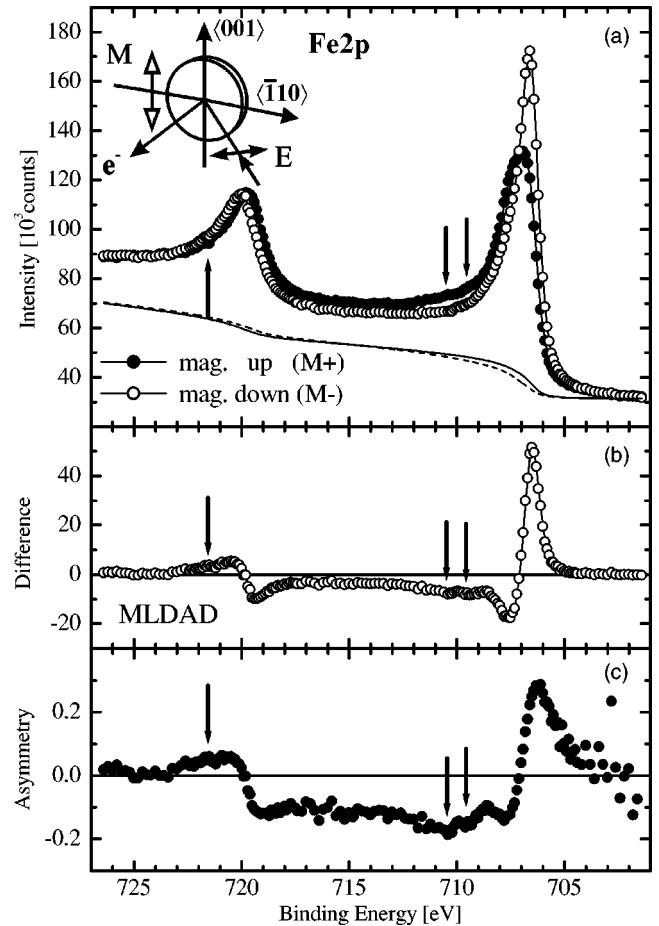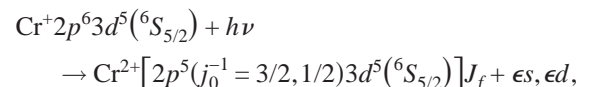


FIG. 1. (a) Fe $2p$ photoemission spectra and Shirley background of 15 ML Fe/W(110) excited with $p$-polarized radiation ($h\nu = 850$ eV) for magnetization up and down (M+, M−). The inset shows the experimental geometry. (b) The intensity difference (MLDAD) of the curves from (a). (c) MLDAD asymmetry (without background). The arrows mark the position of the correlation-induced satellites.

namics of the photoionization process.[18] For a qualitative discussion it is instructive to consider the resulting dipole amplitudes within a pure coupling approximation.[18,19] In deep core-level photoemission the spin-orbit splitting of the core hole dominates the photoemission spectrum and therefore the $jK$ or $jj$ coupling approximations are appropriate.[21]

The $4s$ electrons of the Cr surface layer on Fe in our experiment are itinerant. Therefore the spins of the $4s$ electrons need not be taken into account and the $4s$ shell could be considered as a closed shell. With the nomenclature of Ref. 19, the total angular momentum $j$ of the core hole is denoted as $j_0$. In a first atomic approach the final states of Cr $2p$ photoemission of a submonolayer Cr adsorbate on a thin iron film can be described as the photoionization,

$$Cr^+ 2p^6 3d^5 (^6S_{5/2}) + h\nu$$
$$\rightarrow Cr^{2+} \left[ 2p^5 (j_0^{-1} = 3/2, 1/2) 3d^5 (^6S_{5/2}) \right] J_f + \epsilon s, \epsilon d,$$

in $jj$ coupling. This approximation is based on the assumption that the $2p$ hole states can be characterized by the total
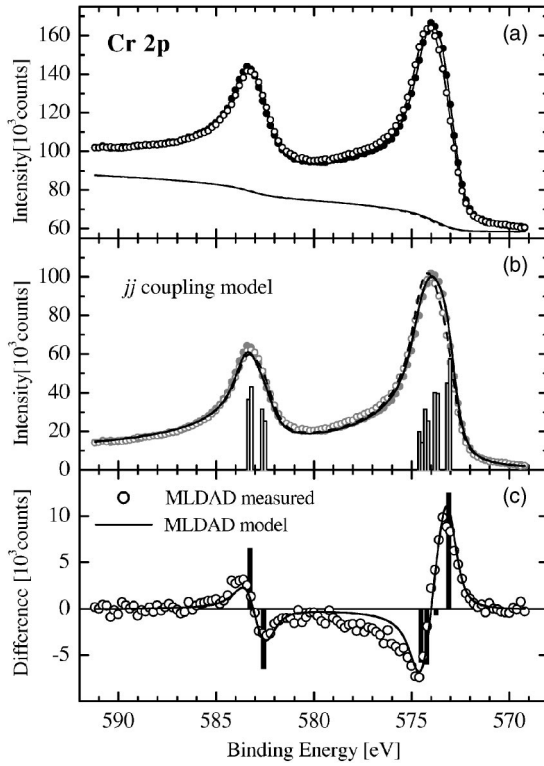
FIG. 2. (a) Cr $2p$ photoelectron spectra of 0.5 ML Cr/Fe/W(110) excited with $p$-polarized radiation ($h\nu=705$ eV) for two opposite magnetizations of the Fe film (Ref. 17). (b) The bar diagram and convoluted line spectrum according to the $jj$ coupling model compared to the measured Cr $2p$ photoelectron spectra after background subtraction. (c) The MLDAD resulting from the measurements (symbols) and our atomic model (line).

angular momentum $j_0=1/2$ and $j_0=3/2$. The interaction of the $2p$ hole and the valence electrons gives rise to a further multiplet splitting. If the valence electrons stay in the Hund's rule ground state ($^6S_{5/2}$) the coupling of the core hole total angular momentum $j_0$ and the total spin of the valence electrons ($S_0=5/2$) results in six final ionic states in two groups with total angular momentum $J_f=3$, 2 for the $j_0=1/2$ and $J_f=1, 2, 3, 4$ for the $j_0=3/2$ core hole.

Figure 2(a) shows the Cr $2p$ photoemission spectra and the appropriate Shirley-type background for opposite magnetic ordered Cr adsorbates of the system 0.5 ML Cr/Fe/Cr/W(110) excited with linearly polarized undulator radiation ($h\nu=750$ eV). Like in previous measurements of this system[16] the Cr adsorbates are coupled antiferromagnetically to the Fe thin film. In Ref. 17 these data were compared to the Cr $2p$ photoionization spectra of free laser-oriented Cr atoms. The multiplet splitting of the $2p$ spectrum of the surface layer is reduced in comparison to that of free Cr atoms, so the spectrum shows less fine structure. This observation is in agreement with other experiments: Studies of $3d$ metal atoms bound in metals have shown that the $2p$-$3d$-Slater integrals are reduced by up to 30% from the scaled free atom values (e.g., Refs. 22 and 23).

Normalizing the MLDAD ($I^{10}$) to the isotropic spectrum ($I^{00}$), the asymmetry is given by $(I(M+)-I(M-))/(I(M+)+I(M-)) \propto \beta_{MLDAD}$. The asymmetry coefficients $\beta$ directly

TABLE I. Fit of relative intensities ($I^{00}$) and MLDAD ($I^{10}$) to the measured Cr $2p$ spectra. The binding energy position of the final states are obtained from Hartree-Fock (HF) calculations on the $2p$ photoionization of $Cr^+$ after a reduction of the Slater-integrals to 50%. The resulting spectra are given in Fig. 2(b).

| Expt. $\pm 0.2$ eV | $j_0$ | $J_f$ | $\Lambda$ (eV) | $\Gamma$ (eV) | $\alpha$ | $I^{00}$ | $I^{10}$ |
|---|---|---|---|---|---|---|---|
| 573.1 | 3/2 | 4 | 0.67 | 0.6 | 0.27 | 9 | 1.10 |
| 573.7 | | 3 | 0.67 | 0.6 | 0.27 | 7 | −0.06 |
| 574.2 | | 2 | 0.67 | 0.6 | 0.27 | 5 | −0.53 |
| 574.5 | | 1 | 0.67 | 0.6 | 0.27 | 3 | −0.51 |
| 582.5 | 1/2 | 2 | 0.94 | 0.6 | 0.27 | 5 | −0.57 |
| 583.3 | | 3 | 0.94 | 0.6 | 0.27 | 7 | 0.57 |

depend on the complex dipole transition amplitudes and therefore describe the dynamics of the photoemission process.[19] A general description of the magnetic dichroism in photoemission from localized magnetic systems is given in Ref. 24. Assuming $LS$ coupling of the initial state and $jj$ coupling of the final state ($j_0$ of the core hole and $J_0$ of the LS-coupled valence electrons) and neglecting the configuration interaction, it is possible to give a simple expression for the MLDAD asymmetry parameter:

$$\beta_{MLDAD} \propto \frac{C_{k_0=1}(j_0,J_f)}{2J_f+1} \frac{R_s R_d \sin(\delta_d - \delta_s)}{R_s^2 + 2R_d^2}. \quad (1)$$

The second factor of the expression is given by the reduced dipole amplitudes $R_s$ and $R_d$ and the relative phases $\delta_s$, $\delta_d$ of the outgoing $\epsilon s$ and $\epsilon d$ electron waves of the one-electron dipole matrix elements $\langle \epsilon l \| d \| l_0 \rangle$. This part is used in the single particle models as well (see van der Laan[3]). The matrix elements and phase shifts have been calculated and tabulated by Goldberg et al.[25] for several elements and energies.

The first factor is the ratio of the MLDAD spectral pattern given by the coupling coefficient $C_{k_0=1}(j_0,J_f)$ and the isotropic spectrum given by the statistical weight $(2J_f+1) \equiv \tilde{I}^{00}$. This ratio can easily be calculated analytically for each multiplet line $(j_0,J_f)$ by the equation

$$C_{k_0}(j_0,J_f) = 3\hat{J}_0 \hat{J}_f^2 \hat{j}_0^2 (-1)^{J_f+J_0+l_0+k_0-1/2} \begin{Bmatrix} j_0 & j_0 & k_0 \\ l_0 & l_0 & \frac{1}{2} \end{Bmatrix}$$
$$\times \begin{Bmatrix} j_0 & j_0 & k_0 \\ J_0 & J_0 & J_f \end{Bmatrix} \quad (2)$$

from Ref. 19 with the standard notations for the Wigner $nj$ coefficients and $\hat{J} \equiv \sqrt{2J+1}$. This part differs from the way the magnetic dichroism is calculated in single particle models.

The results for the six ionic final states $(j_0,J_f)$ are given in Fig. 2(b) as bars. The results and the fit parameter are listed in Table I. The binding energy (BE) position of the final states are obtained from Hartree-Fock (HF) calculations on the $2p$ photoionization of $Cr^+ 3d^5$ after reduction of the Slater-integrals from 85% ($\triangleq$ free atom value[19]) to 50% and

fitted to the measured $(j_0=3/2, J_f=4)$ line. The resulting lines were convoluted with a Doniach-Šunjić (DS) line shape[26] with singularity index $\alpha=0.27$ and Lorentzian broadening $\Lambda_{3/2}=0.67$ eV and $\Lambda_{1/2}=0.94$ eV full width at half maximum (FWHM). The larger width of the $2p_{1/2}$ level is caused by rapid $L_2L_3V$ Coster-Kronig auger processes.[27] The measured spectra (after background subtraction) are added as gray symbols. The experimental Gaussian energy width $\Gamma$ was 0.6 eV. These parameters result in a total FWHM of the two lines of the isotropic spectrum: The $2p_{3/2}$ line has a width of 2.4 eV and the $2p_{1/2}$ line a width of 2.6 eV. Due to our experimental width of about 0.6 eV and the lifetime broadening the resulting fine structure could not be resolved. The difference of the two curves from Fig. 2(b) is given in Fig. 2(c). The symbols were obtained by the difference of the measured data and the solid curve by the difference of the calculated spectra in Fig. 2(b). The relative intensities of the bars are given by $I^{10}$ in Table I. These MLDAD intensities arise directly from the coupling coefficient $C_1(j_0, J_f)$ scaled by the second factor of Eq. (1).

The agreement of the calculated spectra with experiment is generally very good. The observable deviations at 576…579 eV BE can be attributed to many-body effects due to some admixture of other configurations (e.g. $2p^53d^4$) and recoupling of the $3d$ shell.[17]

### B. Fe $2p$ photoemission

Most core level photoelectron spectra of thin Fe films have been discussed in final state models, like the spin-resolved measurements of the Fe $3s$ photoemission for example.[28,29] In a simple "atomic" picture the expected $3d^8$ initial state[28] is giving rise to a doublet low-spin and a quartet high-spin final state $3s^13d^8(^2X,^4X)$. These states were chosen to model the average Fe metal ground state magnetic moment of $2.3\mu_B \approx 2\mu_B$ by the $^3X$ initial state. In this atomic multiplet scheme the intensities of the two final states are proportional to the spin multiplicity of the final states $(2S_f+1)$, separated in energy due to an exchange interaction.[28] The angular momentum of the $3d$ valence electrons is not taken into account. The deviation from the atomic multiplet model reveals the importance of configuration interaction effect of the itinerant $3d$ system.[29]

We will now use the coupling model of this atomic multiplet scheme to describe the Fe $2p$ photoemission spectrum and the MLDAD in the $jj$ coupling model by coupling the total angular momentum $j_0$ of the $2p$ core hole and the total spin $S_0$ of the valence electrons. In case of the Cr $2p$ spectrum we did not take the angular momentum of the valence electrons into account, because even for Cr atoms in the Hund's rule ground state $L_0=0$. The $2p$ photoionization spectrum of Mn atoms can, for the same reasons, also be described by the $jj$ coupling scheme.[20,30] For both elements HF calculations have shown that the $jj$ coupling model reproduces the main features of the $2p$ spectra very well.

The $2p$ photoionization spectrum of Fe atoms in the Hund's rule ground state $[3d^64s^2(^5D_4)]$ shows a much wider splitting of the multiplet lines.[8,31] The $2p_{3/2}$ is split about 5–6 eV, when the Slater-integrals are reduced to the free

atom value. In spite of this large value, the spin-orbit splitting of $\zeta_{Fe}(2p)=8.3$ eV[32] is dominant. Because the angular momentum of the valence electrons is $L_0=2$, the spectrum can be reproduced in the $jK$ coupling scheme better than by $jj$ coupling. In the $jK$ coupling model the number of multiplets is higher as well, because the angular momentum of the $2p$ hole with $j_0$ is first coupled to the $L_0$ of the valence electrons resulting in the angular momentum $K_f$. The $K_f$ then couples with the total spin of the valence electrons $S_0$ to the total angular momentum $J_f$ of the ion. This results in ten ionic final states for $j_0=3/2$ and three ionic final states for $j_0=1/2$ of the Fe($^5D_4$) $2p$ spectrum, mainly grouped by the angular momentum $K_f$. The splitting of the $(j_0, K_f, J_f)$ multiplet lines in the $jK$ coupling model is wider than in the $jj$ coupling scheme due to the magnitude of the Slater parameters $F^2(2p,3d)$ and $G^{1,3}(2p,3d)$, e.g., given in Ref. 32.

The $2p$ photoemission spectra of an Fe film [15 ML Fe/Cr/W(110)] excited with 850 eV linearly $p$-polarized radiation for two opposite magnetizations $(M+, M-)$ are shown in Fig. 1(a). Additionally, the Shirley-type background for both magnetization directions is shown. The difference of the two spectra after background subtraction (i.e., the MLDAD) is displayed in Fig. 1(b), the asymmetry in Fig. 1(c). In contrast to Refs. 28 and 29 we assume a $^4X$ initial state, because the average Fe metal ground state number of majority spin $3d$ electrons per atom is 4.8 and the number of minority spin $3d$ electrons per atom is 2.6. Hence the total number of $3d$ electrons per atom is 7.4. This results in a hybridization of $3d^7$ and $3d^8$ configuration, but we will discuss the spectra assuming just a pure $2p^53d^7$ final state. The results for the $3d^8$ configuration are just little different, and can easily be calculated in the same way by using Eq. (2).

In our case with $^4X$ ground state, the Fe $2p$ photoemission could be described in an atomic model by the photoionization

$$\text{Fe}2p^63d^7(^4X) + h\nu \rightarrow \text{Fe}^+\left[2p^5(j_0^{-1}=3/2,1/2)3d^7(^4X)\right]J_f$$
$$+ \epsilon s, \epsilon d,$$
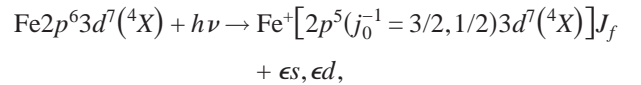
in the $jj$ coupling model. If the valence electrons remain in the ground state $^4X$, the coupling of the core hole total angular momentum $j_0$ and the total spin of the valence electrons $S_0$ results in six final ionic states in two groups with total angular momentum $J_f=2, 1$ for the $j_0=1/2$ and $J_f=0, 1, 2, 3$ for the $j_0=3/2$ core hole.

The results for the four final states with $j_0=3/2$ are given in Fig. 3(a), the two states with $j_0=1/2$ are given in Fig. 4(a) as bars for opposite magnetizations ($M+$ and $M-$). The binding energy position of the final states are figured out by a simple rule of the fine structure of the ionic final states[21] (like Lande's interval rule), slightly varied to obtain the best agreement with measured data, and fitted to the measured $(j_0=3/2, J_f=3)$ line. The multiplet splitting is of the same size as the multiplet splitting of the $2p$ photoemission spectrum of the Cr surface layer shown in Fig. 2.

The resulting multiplet lines of the Fe $2p$ spectrum were convoluted with Doniach-Šunjić line shape[26] with singularity index $\alpha=0.23$ and Lorentzian broadening $\Lambda_{3/2}=0.5$ eV and $\Lambda_{1/2}=1.3$ eV FWHM. The larger width of the $2p_{1/2}$ level is
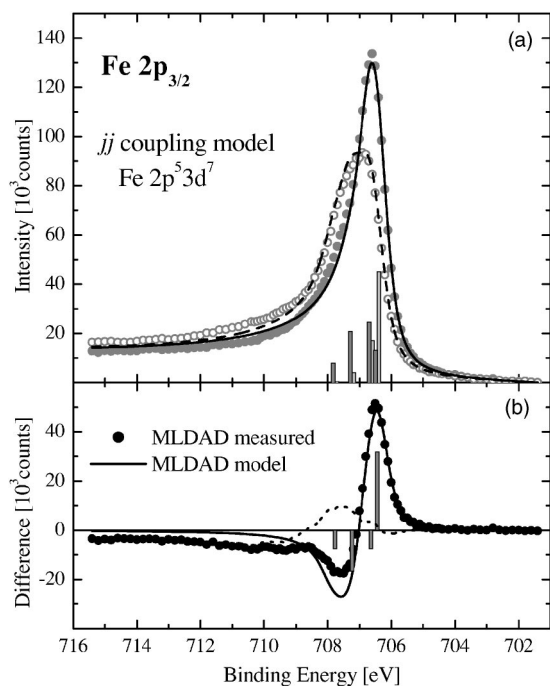
FIG. 3. (a) Fe $2p_{3/2}$ photoemission spectra from Fig. 1. The bar diagram and convoluted line spectrum according to the $jj$ coupling model for $2p^5 3d^7$ final state. Gray symbols: measured spectra after background subtraction. (b) Symbols: MLDAD (difference) from measured data, bars and lines: MLDAD results of the atomic model, dotted line: aberration of measured and calculated MLDAD.
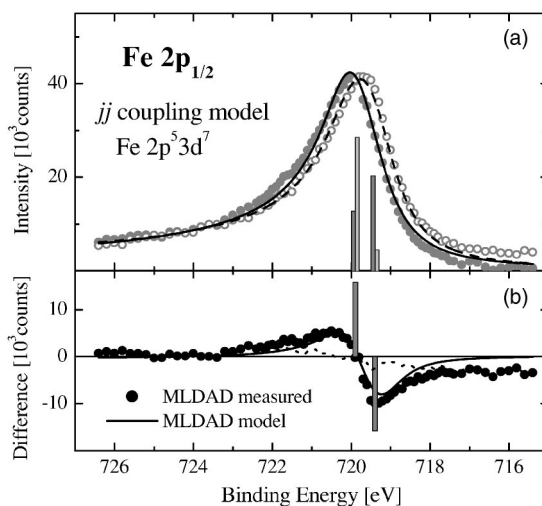


FIG. 4. (a) Fe $2p_{1/2}$ photoemission spectra from Fig. 1. The bar diagram and convoluted line spectrum according to the $jj$ coupling model for $2p^5 3d^7$ final state. Gray symbols: measured spectra after background subtraction. (b) Symbols: MLDAD (difference) from measured data, bars and lines: MLDAD results of the atomic model, dotted line: aberration of measured and calculated MLDAD.

caused by the opening of rapid $L_2 L_3 V$ Coster-Kronig auger decay channels.[27] The measured spectra after background subtraction are added as gray symbols. In Fig. 4(a), the intensity tail of the $2p_{3/2}$ structure is removed as well. The experimental Gaussian energy width $\Gamma$ was about 0.5 eV. These parameters result in a total FWHM of the two lines of the isotropic spectrum: The $2p_{3/2}$ line has a width of 1.7 eV and the $2p_{1/2}$ line a width of 2.3 eV. The difference of the two curves from Figs. 3(a) and 4(a) is given in Figs. 3(b) and 4(b). The curve of symbols was obtained by the difference of the measured data and the solid curve by the difference of the calculated spectra in (a). The relative intensities of the bars are given by $I^{10}$ in Table II. These MLDAD intensities arise directly from the coupling coefficient $C_1(j_0, J_f)$ scaled by a factor considering the dynamics of the photoemission process. Different from the Cr adsorbates on Fe an epitaxial grown 15 ML Fe film shows an explicit influence of photoelectron diffraction, especially on the magnetic dichroism.[33]

The fit shows good agreement with the main structures of the Fe $2p$ photoemission spectra and the MLDAD. On the other hand, the line fit of the $2p_{3/2}$ given in Ref. 7 looks more like the multiplet structure of the above given final state model than what is expected by a one electron model: The intensities of the $2p_{3/2}$ sub-levels are smaller with increasing binding energy. The total splitting of the four lines is higher than the calculated "spin-field" splitting of about 1 eV.[4,6] Additionally two satellite structures of the $2p_{3/2}$ at 709.5 eV and 710.4 eV and one $2p_{1/2}$ satellite at 721.6 eV are observable. They are clearly discernable in the measured spectra and the resulting dichroism in Fig. 1. Although itinerant va-

lence electrons give rise to a statistical binomial distribution over many different $3d^n$ configurations,[11] the number of clearly visible satellite structures is low. The Fe $2p$ satellites are extremely weak because the line strength is transferred from the satellites to the main lines by the screening of additional free valence electrons attracted to the ionized site. This transfer of line strength is more pronounced for final satellite states nearer the main lines.[9] The energy separation of the satellites and the main lines of the $2p$ photoemission spectrum is mainly determined by the on-site $dd$ Coulomb interaction $U$.[11] A comparison of the energy difference of $2p_{3/2}$ main peaks and satellites of the late transition metals (Ni: 5.5 eV,[11] Co: 3.5 eV,[34] and Fe: ~3 eV) shows that the more mobile the $3d$ electrons are, the smaller is this energy difference. Therefore the intensity transfer from the Fe satellite structures to the main lines is stronger than for Co and Ni. For Fe, mainly the hybridization between the configura-

TABLE II. Fit of relative intensities ($I^{00}$) and MLDAD ($I^{10}$) to the measured Fe $2p$ spectra. The binding energy position of the final states is figured out by a simple rule of the fine structure of the ionic final states (Ref. 21) and slightly varied, to obtain the best agreement with measured data. The resulting spectra are given in Fig. 3 and Fig. 4.

| Expt. $\pm 0.2$ eV | $j_0$ | $J_f$ | $\Lambda$ (eV) | $\Gamma$ (eV) | $\alpha$ | $I^{00}$ | $I^{10}$ |
|---|---|---|---|---|---|---|---|
| 706.45 | 3/2 | 3 | 0.5 | 0.5 | 0.23 | 7 | 3.83 |
| 706.65 | | 2 | 0.5 | 0.5 | 0.23 | 5 | −0.91 |
| 707.25 | | 1 | 0.5 | 0.5 | 0.23 | 3 | −2.01 |
| 707.75 | | 0 | 0.5 | 0.5 | 0.23 | 1 | −0.91 |
| 719.4 | 1/2 | 1 | 1.3 | 0.5 | 0.23 | 3 | −1.82 |
| 719.9 | | 2 | 1.3 | 0.5 | 0.23 | 5 | 1.82 |

TABLE III. Coupled wavefunctions $|j_0 S_0 : J_f\rangle$ of the six ionic final states of $Fe(2p^5 3d^7)^+$ in the framework of the $jj$ coupling model with $m_{S_0} = +3/2$. The expectation values $\langle m \rangle$ and $\langle \sigma \rangle$ from $|j_0 S_0 : J_f\rangle$ and $|j_0 m_{j_0}\rangle$ as linear combinations of $|lm\rangle|s\sigma\rangle$. The coupling coefficient $C_1$ [from Eq. (2)] is $\sqrt{2/5}\, C_1 = (2J_f+1)\langle m \rangle$ with $I^{00} \propto (2J_f+1) = \tilde{I}^{00}$.

| $j_0$ | $J_f$ | $\|j_0 S_0 : J_f\rangle$ as linear combination of $\|j_0 m_{j_0}\rangle\|S_0(m_{S_0} = +\frac32)\rangle$ | $\langle m \rangle$ | $\langle \sigma \rangle$ | $\tilde{I}^{00}\langle m \rangle$ | $C_{k_0=1}$ | $\tilde{I}^{00}\langle \sigma \rangle$ |
|---|---|---|---|---|---|---|---|
| $\frac32$ | 3 | $\left(\frac{\sqrt{700}}{35}\|\frac32+\frac32\rangle + \frac{\sqrt{350}}{35}\|\frac32+\frac12\rangle + \frac{\sqrt{140}}{35}\|\frac32-\frac12\rangle + \frac{\sqrt{35}}{35}\|\frac32-\frac32\rangle\right)\|\frac32+\frac32\rangle$ | $\frac35(+1)$ | $\frac35(1\downarrow)$ | $+\frac{21}{5}$ | $+\sqrt{\frac{441}{10}}$ | $+\frac{21}{5}$ |
| | 2 | $\left(-\frac{\sqrt{10}}{5}\|\frac32+\frac12\rangle - \frac{\sqrt{10}}{5}\|\frac32-\frac12\rangle - \frac{\sqrt5}{5}\|\frac32-\frac32\rangle\right)\|\frac32+\frac32\rangle$ | $-\frac35(+\frac13)$ | $-\frac35(\frac13\downarrow)$ | $-1$ | $-\sqrt{\frac52}$ | $-1$ |
| | 1 | $\left(\frac{\sqrt{25}}{5}\|\frac32-\frac12\rangle + \frac{\sqrt{10}}{5}\|\frac32-\frac32\rangle\right)\|\frac32+\frac32\rangle$ | $\frac{11}{5}(-\frac13)$ | $\frac{11}{5}(\frac13\uparrow)$ | $-\frac{11}{5}$ | $-\sqrt{\frac{121}{10}}$ | $-\frac{11}{5}$ |
| | 0 | $-\|\frac32-\frac32\rangle\|\frac32+\frac32\rangle$ | $1(-1)$ | $1(1\uparrow)$ | $-1$ | $-\sqrt{\frac52}$ | $-1$ |
| $\frac12$ | 1 | $-\|\frac12-\frac12\rangle\|\frac32+\frac32\rangle$ | $1(-\frac23)$ | $1(\frac13\downarrow)$ | $-2$ | $-\sqrt{10}$ | $+1$ |
| | 2 | $\left(\frac{\sqrt{20}}{5}\|\frac12+\frac12\rangle + \frac{\sqrt5}{5}\|\frac12-\frac12\rangle\right)\|\frac32+\frac32\rangle$ | $\frac35(+\frac23)$ | $\frac35(\frac13\uparrow)$ | $+2$ | $+\sqrt{10}$ | $-1$ |

tions in the remaining final state main line is vital to describe the $2p$ photoemission spectrum. The results of this hybridization are close to the assumed $2p^5 3d^7$ final state.

The model which we use here is based on pure coupling approximation ($jj$ or $jK$ coupling). It implies the sum rule that the dichroism vanishes for each $j_0$ substructure when it is integrated over the $J_f$ fine structure. Therefore the calculated MLDAD at 707.6 eV is larger than the measured dichroism. The deviation of the MLDAD spectra given in Fig. 3(b) as a dotted line can be discussed similar to the Ni $2p$ spectra:[9] The negative MLDAD lobe of the $2p_{3/2}$ main line is diluted by the positive MLDAD of the $2p_{3/2}$ satellite structures at 709…711 eV. As we will discuss below, the positive magnetic dichroism of the $2p_{3/2}$ is linked to minority spin polarization. The satellites have a remaining net majority spin polarization (see Hillebrecht *et al.*[7]), leading to the negative MLDAD in the $2p_{3/2}$ satellite structure and the positive MLDAD in the $2p_{1/2}$ satellite structure.

The relation between spin polarization and magnetic dichroism is often discussed in a single particle model,[4–7] sometimes even when the spectrum itself is discussed in a final state model.[11] We will now show that a discussion in the $jj$ coupling model leads to analog results.

In the single particle model $m_j$ is assumed to be a proper quantum number to characterize the sub-levels of the Fe $2p$ spectrum.[3–6] The exchange interaction of the spin polarized $3d$ valence electrons and the $2p$ core electrons causes a splitting $m_j = -1/2$, $1/2$ with dichroism $2\Delta$, $-2\Delta$ for the $j=1/2$ and $m_j = 3/2$, $1/2$, $-1/2$, $-3/2$ with dichroism $-3\Delta$, $-\Delta$, $+\Delta$, $+3\Delta$ for the $j=3/2$ level with nearly equidistant splitting $\Delta E = \xi/3$. The spin-field giving the split of the sub-levels $m_j = \pm 3/2$ is about $\xi = 0.8…1.2$ eV.[3–6] The wavefunction of the six states $|j, m_j\rangle$ is given as a linear combination of $|l, m\rangle |s, \sigma\rangle$ ("$m\sigma$ states" in Table IV of Ref. 3). These $|j, m_j\rangle$ spin-orbit states can be constructed directly from the Clebsch-Gordan coefficients. For strong spin-orbit coupling, like at the Fe $2p$ level, the dichroism pattern arises from $\langle m \rangle$ and the spin pattern from $\langle \sigma \rangle$. In the limit of $jj$ coupling ($\zeta \gg \xi$) we have

$$\langle m \rangle = 2\langle l \cdot s \rangle \langle \sigma \rangle, \qquad (3)$$

where the polarization $\langle l \cdot s \rangle$ is $1/2$ for $2p_{3/2}$ and $-1$ for $2p_{1/2}$.[11] With Eqs. (4) and (5) of Ref. 11: $I^{10} = -2I^{01}$ for $j$

$=1/2$ and $I^{10} = I^{01}$ for $j=3/2$. The spin resolved Fe $2p$ photoemission measurements of Hillebrecht *et al.*[7] confirm the relation of the $I^{10}$ and the $I^{01}$ spectrum for $j=3/2$. Because of the DS lineshape and $2p_{3/2}$ satellite structures between the main lines a separation of "pure" states with $j=1/2$ is difficult, but the reversed sign of $I^{10}$ and $I^{01}$ is clearly visible in Ref. 7. On the other hand, the experiment showed that the measured Fe $2p$ spectrum and the magnetic dichroism cannot be explained correctly by the one electron model.

Finally, we consider whether $m_j$ is a good quantum number in the atomic final state model as well. For this purpose we calculated the coupled wavefunctions $|j_0 S_0 : J_f\rangle$ of the six ionic final states of $Fe^+ 2p^5 3d^7$ in the framework of the above established $jj$ coupling model with $m_{S_0} = +3/2$ shown in Table III. To keep the results clear, we limited $m_{S_0}$ of the $3d$ electrons to the maximum value. Only the multiplet lines ($j_0 = 3/2$, $J_f = 0$) and ($j_0 = 1/2$, $J_f = 1$) consist of pure $|j_0, m_{j_0}\rangle$ states. The other four multiplet lines ($j_0 = 3/2$, $J_f = 3, 2, 1$ and $j_0 = 1/2$, $J_f = 2$) are composed of multiple $|j_0, m_{j_0}\rangle$ states. The expectation values $\langle m \rangle$ and $\langle \sigma \rangle$ are evaluated for each multiplet similarly to the single particle approach by calculating the $|j_0 m_{j_0}\rangle$ components as linear combination of $|lm\rangle |s\sigma\rangle$. The values of $\langle m \rangle$ and $\langle \sigma \rangle$ given in Table III are comparable to the values of the six adequate states of the single particle model.[3–7] Although the symmetry $I^{10}(j, m_j) = -I^{10}(j, -m_j)$ of the dichroism in a single particle model is broken, the relation between $\langle m \rangle$ and $\langle \sigma \rangle$ given in Eq. (3) is valid for each final state multiplet component in our example in the $jj$ coupling model.

Further on, Table III shows that the factor $\tilde{I}^{00}\langle m \rangle$ with the statistical weight $\tilde{I}^{00} \equiv (2J_f+1)$ is proportional to the coupling coefficient $C_{k_0=1}(j_0, J_f)$. Therefore $\tilde{I}^{00}\langle m \rangle$ is proportional to the MLDAD $I^{10}$ for each ($j_0, J_f$) multiplet in the $jj$ coupling scheme. According to this rule the spin pattern $\tilde{I}^{00}\langle \sigma \rangle$ are proportional to the spin spectrum $I^{01}$. From Table III one can see that the relations $I^{10} = -2I^{01}$ for each multiplet of $j_0 = 1/2$ and $I^{10} = I^{01}$ for each multiplet of $j_0 = 3/2$ is valid for the final state model with $jj$ coupling as well.

## IV. CONCLUSIONS

Due to the close correspondence between the magnetic dichroism in the 2*p* photoelectron spectra of a Cr surface layer (antiferro-)magnetically coupled to a Fe film and free laser oriented Cr atoms,[17] the 2*p* spectra of a Cr surface layer are well reproduced by a simple "atomic" model based on *jj* coupling. This model is transferred to describe the Fe 2*p* photoemission spectrum of a thin Fe film. Assuming a single-configuration, and pure *jj* coupling scheme, the calculated spectra and the resulting magnetic dichroism in the main structures are in good agreement with experiment. The origin of the MLDAD $(+--+)$ patterns of the main lines can be traced back to the multiplet splitting in the final state. This demonstrates the importance of the 2*p*-3*d* Coulomb and exchange interaction in the 2*p* photoemission of 3*d* metal films. Additional satellite structures are observable. They can be attributed to many-body effects due to the admixture of other configurations.

On the other hand, the atomic final state model shows similarity to the single particle model, although the origin of both effects is different: In the single particle model it is assumed that the exchange interaction of the 2*p* core electrons and the spin-polarized itinerant 3*d* valence electrons in the ground state causes a Zeeman-like splitting of the $2p_{3/2}$ and $2p_{1/2}$ into $m_j$ sublevels. The 2*p* photoemission spectra in the final state model are governed by multiplet splitting and satellite appearance. These features are given by the interaction of the core hole with the valence electrons and the electronic structure of the valence electrons within the solid. The dichroism in both models is described by a photoemission probability of the respective sublevels depending on the radiation polarization. For all these differences, the correlation between magnetic dichroism and spin orbit and exchange induced spin polarization is equal in both models, if a well-defined single initial state is presumed.

*Electronic address: bethkec@uni-duesseldorf.de

[1] D. G. Van Campen, R. J. Pouliot, and L. E. Klebanoff, Phys. Rev. B **48**, 17 533 (1993).

[2] L. Baumgarten, C. M. Schneider, H. Petersen, F. Schäfers, and J. Kirschner, Phys. Rev. Lett. **65**, 492 (1990).

[3] G. van der Laan, Phys. Rev. B **51**, 240 (1995).

[4] H. Ebert, L. Baumgarten, C. M. Schneider, and J. Kirschner, Phys. Rev. B **44**, 4406 (1991).

[5] J. G. Menchero, Phys. Rev. B **57**, 993 (1998).

[6] J. Henk, A. M. N. Niklasson, and B. Johansson, Phys. Rev. B **59**, 13 986 (1999).

[7] F. U. Hillebrecht, C. Roth, H. B. Rose, W. G. Park, E. Kisker, and N. A. Cherepkov, Phys. Rev. B **53**, 12 182 (1996).

[8] B. T. Thole and G. van der Laan, Phys. Rev. B **44**, 12 424 (1991).

[9] J. G. Menchero, Phys. Rev. Lett. **76**, 3208 (1996).

[10] J. G. Menchero, Phys. Rev. B **55**, 5505 (1997).

[11] G. van der Laan, S. S. Dhesi, and E. Dudzik, Phys. Rev. B **61**, 12277 (2000).

[12] C. De Nadaï, G. van der Laan, S. S. Dhesi, and N. B. Brookes, Phys. Rev. B **68**, 212401 (2003).

[13] G. van der Laan, S. S. Dhesi, E. Dudzik, J. Minar, and H. Ebert, J. Phys.: Condens. Matter **12**, L275 (2000).

[14] H. A. Dürr, G. van der Laan, D. Spanke, F. U. Hillebrecht, and N. B. Brookes, Europhys. Lett. **40**, 171 (1997); H. A. Dürr, G. van der Laan, D. Spanke, F. U. Hillebrecht, and N. B. Brookes, J. Electron Spectrosc. Relat. Phenom. **93**, 233 (1998).

[15] G. Gradmann and G. Waller, Surf. Sci. **116**, 539 (1982).

[16] D. Knabben, T. Koop, H. A. Dürr, F. U. Hillebrecht, and G. van der Laan, J. Electron Spectrosc. Relat. Phenom. **86**, 201 (1997).

[17] P. Wernet, J. Schulz, B. Sonntag, K. Godehusen, P. Zimmermann, M. Martins, C. Bethke, and F. U. Hillebrecht, Phys. Rev. B **62**, 14331 (2000).

[18] A. Verweyen, A. N. Grum-Grzhimailo, and N. M. Kabachnik, Phys. Rev. A **60**, 2076 (1999).

[19] P. Wernet, J. Schulz, B. Sonntag, K. Godehusen, P. Zimmermann, A. N. Grum-Grzhimailo, N. M. Kabachnik, and M. Martins, Phys. Rev. A **64**, 042707 (2001).

[20] P. Wernet, B. Sonntag, M. Martins, P. Glatzel, B. Obst, and P. Zimmermann, Phys. Rev. A **63**, 050702(R) (2001).

[21] R. D. Cowan, *The Theory of Atomic Structure and Spectra* (University of California Press, Berkeley, 1981).

[22] J. Fink, T. Müller-Heinzerling, B. Scheerer, W. Speier, F. U. Hillebrecht, J. C. Fuggle, J. Zaanen, and G. A. Sawatzky, Phys. Rev. B **32**, 4899 (1985).

[23] F. M. F. de Groot, J. C. Fuggle, B. T. Thole, and G. A. Sawatzky, Phys. Rev. B **42**, 5459 (1990).

[24] B. T. Thole and G. van der Laan, Phys. Rev. B **49**, 9613 (1994).

[25] S. Goldberg, C. Fadley, and S. Kono, J. Electron Spectrosc. Relat. Phenom. **21**, 285 (1981).

[26] S. Doniach and S. Šunjić, J. Phys. C **3**, 285 (1970).

[27] A. L. R. Nyholm, N. Mårtensson, and U. Axelsson, J. Phys. F: Met. Phys. **11**, 1727 (1981).

[28] T. Kachel, C. Carbone, and W. Gudat, Phys. Rev. B **47**, 15 391 (1993).

[29] K.-H. Park, S.-J. Oh, K. Shimada, A. Kamata, K. Ono, A. Kakizaki, and T. Ishii, Phys. Rev. B **53**, 5633 (1996).

[30] K. Godehusen, P. Wernet, T. Richter, P. Zimmermann, and M. Martins, Phys. Rev. A **68**, 052707 (2003).

[31] T. Richter, K. Godehusen, M. Martins, T. Wolff, and P. Zimmermann, Phys. Rev. Lett. **93**, 023002 (2004).

[32] G. van der Laan and I. W. Kirkman, J. Phys.: Condens. Matter **4**, 4189 (1992).

[33] R. Schellenberg, E. Kisker, A. Fanelsa, F. U. Hillebrecht, J. G. Menchero, A. P. Kaduwela, C. S. Fadley, and M. A. Van Hove, Phys. Rev. B **57**, 14 310 (1998).

[34] G. Panaccione, G. van der Laan, H. A. Dürr, J. Vogel, and N. B. Brookes, Eur. Phys. J. B **19**, 281 (2001).